

Finite element modelling and updating of friction stir welding (FSW) joint for vibration analysis

Siti Norazila Zahari¹, Mohd Shahrir Mohd Sani^{1,2,} and Mahadzir Ishak²*

¹Advanced Structural Integrity and Vibration Research (ASIVR), Faculty of Mechanical Engineering, Universiti Malaysia Pahang, 26600 Pekan, Pahang, Malaysia

²Automotive Engineering Centre, Universiti Malaysia Pahang, Malaysia

Abstract. Friction stir welding of aluminium alloys widely used in automotive and aerospace application due to its advanced and lightweight properties. The behaviour of FSW joints plays a significant role in the dynamic characteristic of the structure due to its complexities and uncertainties therefore the representation of an accurate finite element model of these joints become a research issue. In this paper, various finite elements (FE) modelling technique for prediction of dynamic properties of sheet metal jointed by friction stir welding will be presented. Firstly, nine set of flat plate with different series of aluminium alloy; AA7075 and AA6061 joined by FSW are used. Nine set of specimen was fabricated using various types of welding parameters. In order to find the most optimum set of FSW plate, the finite element model using equivalence technique was developed and the model validated using experimental modal analysis (EMA) on nine set of specimen and finite element analysis (FEA). Three types of modelling were engaged in this study; rigid body element Type 2 (RBE2), bar element (CBAR) and spot weld element connector (CWELD). CBAR element was chosen to represent weld model for FSW joints due to its accurate prediction of mode shapes and contains an updating parameter for weld modelling compare to other weld modelling. Model updating was performed to improve correlation between EMA and FEA and before proceeds to updating, sensitivity analysis was done to select the most sensitive updating parameter. After perform model updating, total error of the natural frequencies for CBAR model is improved significantly. Therefore, CBAR element was selected as the most reliable element in FE to represent FSW weld joint.

1 Introduction

Friction stir welding (FSW) is rapidly used to join thin sheet metal with similar and dissimilar materials in the application of shipbuilding, aerospace, railway and automotive [1-3]. FSW seems to be prominent technique as its enable to join dissimilar materials in solid state while avoiding drawbacks of fusion welding due to the large difference in terms

* Corresponding author: mshahrir@ump.edu.my

of chemical composition and physical properties between the components to be joined. FSW joints not only provide connection between sheet metal but also significantly influence the global structural behaviour of complete structures. Therefore, it is crucial to understand the dynamics characteristics of the welded joints which can be achieved via computational and experimental work. Even though prediction task through computational methods are widely used in predicting the behaviour of welds on a complete structure, developing a numerical model of the weld itself is a complex issue. This is mainly because of the existence of many local effects that are not taken into account by FE modelling when predicting frequencies and modes.

Recent years, many works regarding on FSW in dissimilar materials such as dissimilar alloy [4-6] focusing more on microstructure and mechanical properties of the weld itself. There have been several studies in the literature reporting on modelling of FSW [7-11] concentrated in simulation of the process and limit capacity analysis. Modelling for these types of analysis required detailed mesh in order to work out a smooth stress field within and around FSW weld joint. On the contrary for vibration analysis, only simplified model which represent the stiffness of FSW weld and enable predict their influence for entire structure [12]. To the author's best knowledge, there is no reported work on modelling the dynamic behaviour of a structure with FSW welded structure. For the dynamic analysis of FSW welded structures, a major requirement of FSW finite element models is to accurately predict the dynamic characteristics of welded structures with a small number of degrees of freedom. Previous research has reported not taking into consideration the effect of welded joints in their mode [13]. For instance, Sani [13] investigated on identification of dynamics modal parameter for car chassis. A rigid connection was assumed at the welded joint in the car chassis.

The primary goal of this study is to present an appropriate way on how to model FSW welded joints between dissimilar materials using finite element method. In this paper, AA6061 and AA7075 Al alloy used as the base material due to its significant application in automotive, rail transportation and aerospace industries.

First, the welded joint will be modelled using equivalent technique as an initial model and result from numerical analysis will be compared using nine set of experimental results in order to choose the most ideal set of FSW welded plate. Then, three types of modelling technique using rigid body connection element, single bar element and spot weld connection; CWELD will be discussed. All types of FE modelled will undergo normal mode analysis and the predicted result will be validated using experimental modal analysis (EMA) to select the most reliable model to represent FSW joint. Model updating will be carried out for selected to improve correlation between experiment and numerical counterparts.

2 Description of structure

2.1 Material specification and welding process

Nine specimens consists of two different series of aluminium alloy plates; AA6061 and AA7075 with the same dimensions (200 mm × 100 mm × 2 mm) as illustrated in Figure 1 jointed together by FSW. The joint configuration for this paper is square butt joint, where its being joined together using tool pin that transverse along longitudinal length at the centre point between two plates. Tool steel with material AISI H13 with cylindrical pin profile was used as welding tool [14]. The tool consists of shoulder and pin with diameter 17.7 mm and 5.80 mm for each. Backing plate and parallel bar were made of mild steel used to support and hold the specimen during welding process.

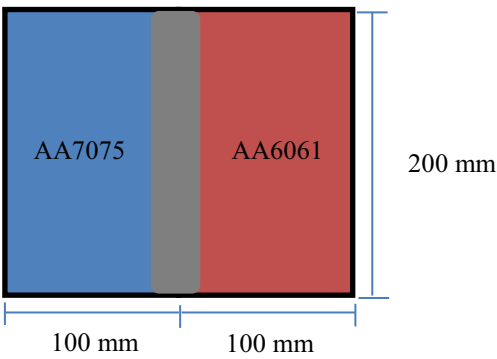


Fig. 1. Two plates with dissimilar material welded by FSW.

FSW process was carried out using vertical milling machine. For this study, plate AA6061 was placed on advancing side [4, 15] due to its higher mechanical strength and tool pin was positioned at the center of joint line. Process parameters used in this study are tabulated in Table 1. Figure 2 below show the specimen after being welded.

Table 1. Welding parameters.

| | Rotational Speed (rpm) | Welding Speed (mm/min) | Tilt Angle (°) |
|---|---------------------------|---------------------------|----------------|
| A | 900 | 30 | 0 |
| B | 1000 | 30 | 1 |
| C | 1100 | 30 | 2 |
| D | 900 | 40 | 0 |
| E | 1000 | 40 | 1 |
| F | 1100 | 40 | 2 |
| G | 900 | 50 | 0 |
| H | 1000 | 40 | 1 |
| I | 1100 | 50 | 2 |

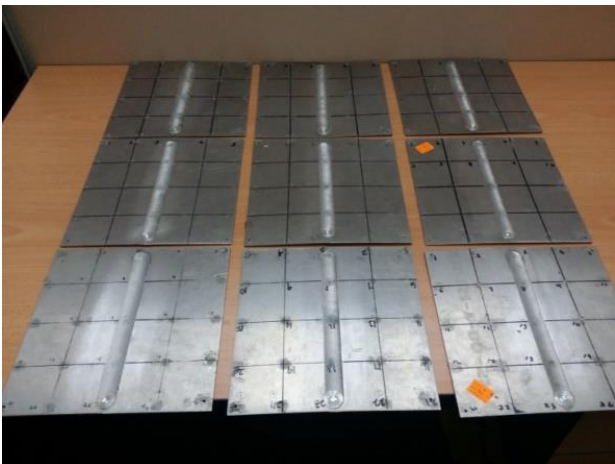


Fig. 2. Nine set of specimens.

3 Experimental modal analysis

Modal testing was executed to extract modal parameters such as natural frequency and mode shapes experimentally. Impact hammer testing used as excitation method in this EMA. The plate was supported by a sponge in order to achieve free-free boundary conditions. The experiment setup is illustrated in Figure 3 below.

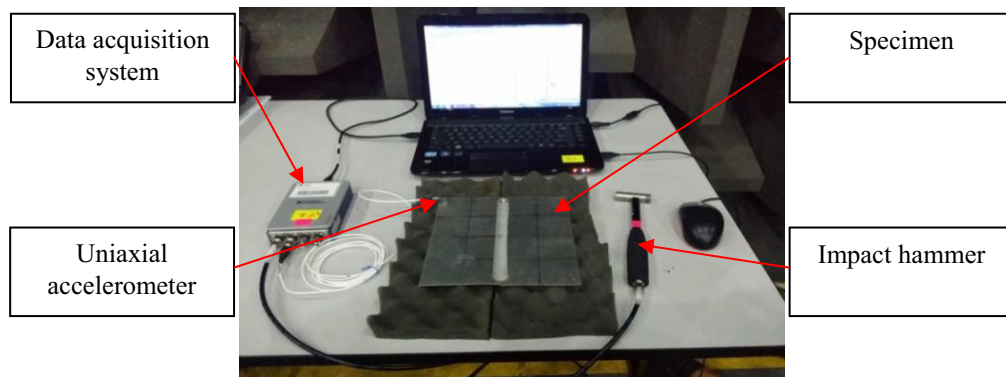


Fig. 3. Experimental modal analysis setup.

The welded plates were divided into 25 small grids points to obtain frequency response function (FRF). A PCB Piezotronic uniaxial accelerometer with sensitivity of 97.17mV/g was used in this experiment and it roved to each of 25 points shown in this test. The structure is excited by an impact hammer fixated at point 14 on the specimen. The excitation force and the response accelerations are acquired and analyzed using the FFT analyzer. Then the FRFs are calculated. Modal parameters (natural frequency and mode shapes) extracted using curve fitting method in MEscape software and results tabulated in the Table 2 below as validation of numerical result.

4 Finite element model and analysis (FEA) for initial model

A commercial finite element software package namely, MSC Patran was used to model the specimen with FSW joint and MSC Nastran was utilized to generate its natural frequency and mode shapes using normal mode analysis (SOL103). A FE model of the structure shown in Figure 1 is built using four noded shell elements (CQUAD4). Neither constraints nor load were assigned to create free-free boundary state. Minimum frequency of 1Hz being set to avoid the solver from calculating the six rigid body motions that having frequency less than 1 Hz. The materials for two flat plates are assigned according to their properties. Material AA6061 have density, ρ of 2700 kg/m³ with Young modulus, E of 69 GPa. The density for material AA7075 is 2820 kg/m³ and Young modulus of 72 GPa. Initial model using equivalence nodes had been developed in order the select the most optimum specimen that can be used later for another FSW modelling technique.

4.1 Material specification and welding process

When the structure consists of more than one surface, use of equivalence becomes mandatory in order to connect the mesh. The equivalence command in MSC Patran plays a role as remover of redundant node between two surfaces. Figure 4 present the details on equivalence nodes in connecting the two surfaces and represent the rigid connection between them and neglecting the joint connection that exist.

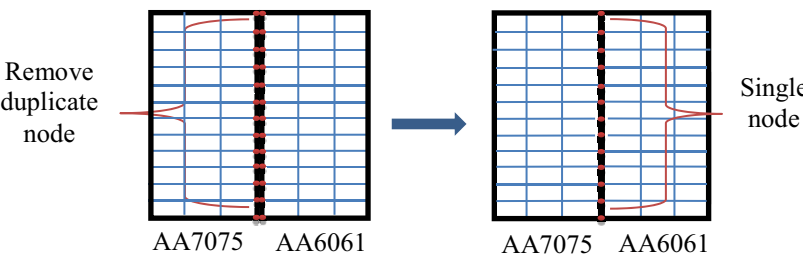


Fig. 4. Equivalence node.

4.2 Finite element analysis (FEA) of initial model

Normal mode analysis (SOL 103) in MSC NASTRAN was performed to compute the modal data of the FSW welded structure.

4.3 Comparison between EMA and FEA for initial model

Natural frequency from the experimental are compared with the natural frequency of FEA and being listed in Table 2 and Table 3 show the percentage error of nine set of specimen and Figure 5 presents the mode shape extracted from numerical and test analysis.

Table 2. FEA vs EMA for nine set of specimen (natural frequency).

| Natural Frequency (Hz) | | | | | | | | | |
|------------------------|-----------|-----|-----|-----|-----|-----|-----|-----|-----|
| FEA | EMA (SET) | | | | | | | | |
| | A | B | C | D | E | F | G | H | I |
| 160.12 | 144 | 178 | 154 | 158 | 143 | 162 | 154 | 143 | 168 |
| 232.19 | 190 | 235 | 240 | 203 | 232 | 208 | 200 | 217 | 260 |
| 296.01 | 298 | 260 | 316 | 308 | 308 | 286 | 329 | 301 | 326 |
| 406.47 | 398 | 402 | 364 | 426 | 432 | 398 | 396 | 345 | 363 |
| 413.80 | 458 | 422 | 444 | 450 | 437 | 472 | 538 | 424 | 436 |

Table 3. Percentage of error between FEA and EMA.

| Natural Frequency (Hz) | | | | | | | | | |
|------------------------|-----------|-------|-------|-------|-------|-------|-------|-------|-------|
| FEA | EMA (SET) | | | | | | | | |
| | A | B | C | D | E | F | G | H | I |
| 160.12 | 11.19 | 10.04 | 3.97 | 1.34 | 11.97 | 1.16 | 3.97 | 11.97 | 4.69 |
| 232.19 | 22.21 | 1.20 | 3.25 | 14.38 | 0.08 | 11.63 | 16.10 | 7.00 | 10.70 |
| 296.01 | 0.67 | 13.85 | 6.33 | 3.89 | 3.89 | 3.50 | 10.03 | 1.66 | 9.20 |
| 406.47 | 2.13 | 1.11 | 11.67 | 4.58 | 5.91 | 2.13 | 2.64 | 17.82 | 11.98 |
| 413.80 | 9.65 | 1.94 | 6.80 | 8.04 | 5.31 | 12.33 | 23.09 | 2.41 | 5.09 |
| Total Error | 45.85 | 28.14 | 32.02 | 32.23 | 27.16 | 30.75 | 55.83 | 40.86 | 41.66 |

Table 3 indicates that set E have the minimum total error between FEA and EMA. These findings provide evidence that Set E represent the ideal joint condition compare to other set of specimen. Therefore, Set E will undergo other modelling technique to find the most suitable method to represent this specimen.

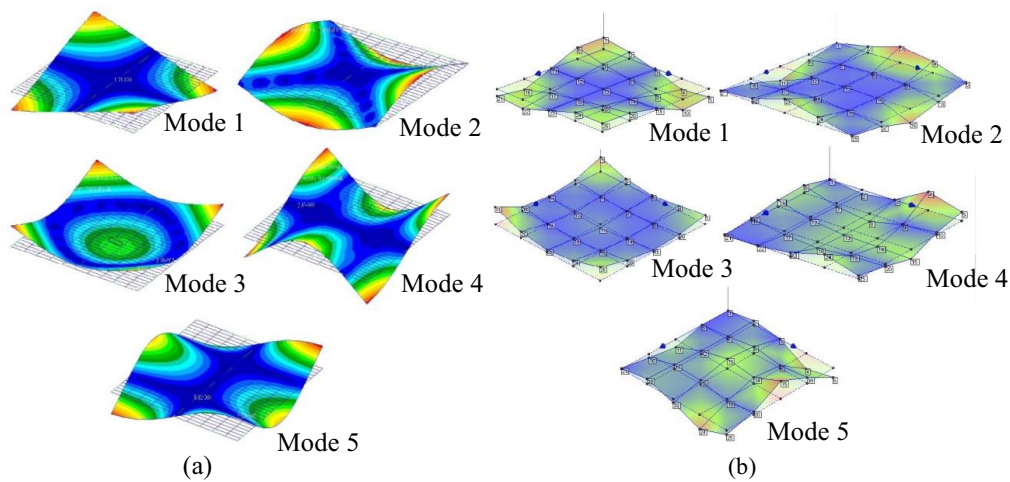


Fig. 5. Mode shapes from (a) FEA and (b) EMA.

5 Different approach of finite element model technique of FSW

This section discusses the details on the other technique for modelling the FSW weld joints for Set E using rigid body element (RBE2), one dimensional bar element and CWELD element.

5.1 Rigid Body Element (RBE2)

Rigid body with independent degree of freedom (DOF) at one grid and dependent DOF at an arbitrary number of grids called RBE2. These elements rigidly weld multiple grids to other grid.

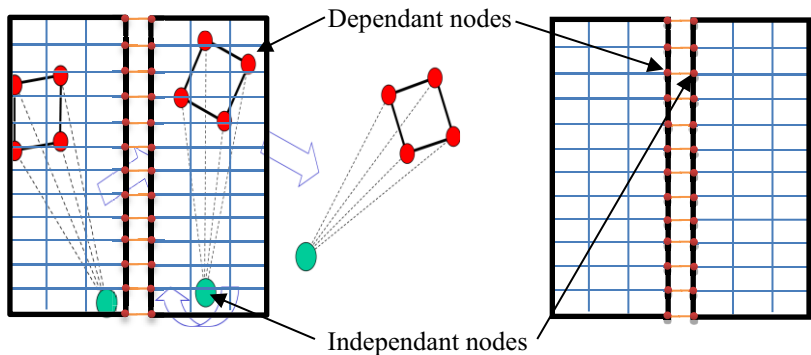


Fig. 6. RBE2.

In modelling the welded flat plate, 31 RBE2 elements being assigned with the middle nodes of each plate attached to one another in a straight line [16]. The first five frequencies of the FE model with RBE2 weld joint representative are tabulated in Table 4 (column III) and the FE results are validated by comparing them with their experimental counterparts.

5.2 One dimensional (1D) bar element (CBAR)

31 curves had been assigned to connect the two plates as shown in Figure 7. Bar element defined as a type of properties for curve. The diameter for bar is 0.018m and its geometrical properties; Young modulus, density and Poisson ratio had been set same as base material.

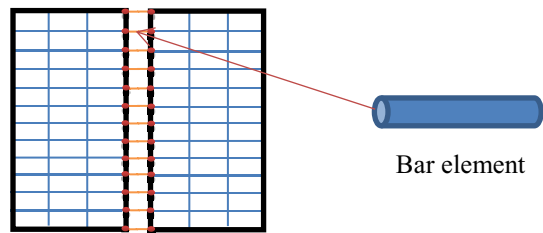


Fig. 7. CBAR element.

5.3 Spot weld connector element - CWELD

The CWELD element (Figure 8) is developed using a two noded special shear flexible beam type element with 12 DOFs (six for each node) and each node is connected to its corresponding patch with constraints from the Kirchhoff shell theory [17].

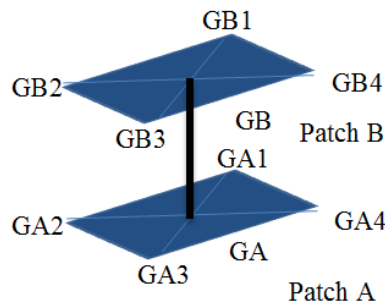


Fig. 8. CWELD element.

In modelling the FSW weld joints, 16 CWELD elements are employed to represent continuous weld at the center of adjacent edge of two plates. The property of CWELD element defined on a PWELD entry. The diameter of spot weld being set approximately 18 mm equals to diameter of tool shoulder that been used in FSW.

5.4 Comparison of EMA and FEA and selection of elements representing FSW joints

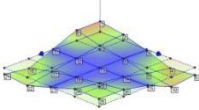
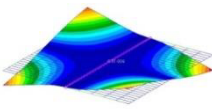
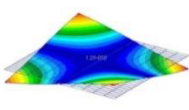
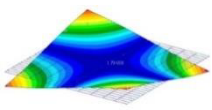
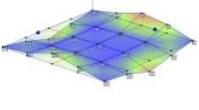
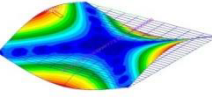
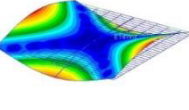
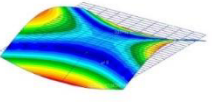
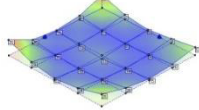
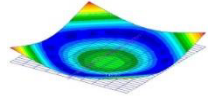
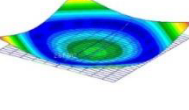
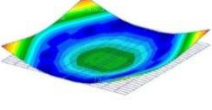
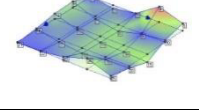
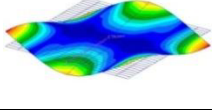
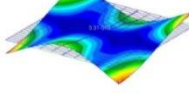
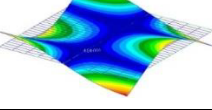
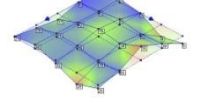
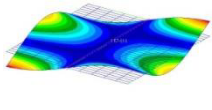
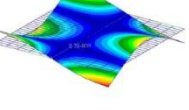
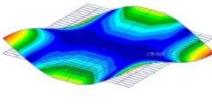
The three types of model are compared in order to choose the most reliable to represent FSW joints. Table 4 summarized the percentage of error of RBE2, CBAR and CWELD while Table 5 illustrated the prediction of mode shape.

From the result, it shows that CBAR suffering of underestimation of natural frequency meanwhile CWELD element and RBE2 capable to reduce the percentage error. However based on Table 5 for prediction of mode shapes, mode swapping problem occurred for mode 4 and 5 when utilizing the CWELD element. In contrast, the mode shapes are successfully predicted by RBE2 and CBAR element.

Table 4. Percentage of error between EMA and FEA for 3 types of modelling.

| Modes | Natural Frequency (Hz) | | | | | | |
|--------------------|------------------------|--------|----------------------|--------|----------------------|--------|----------------------|
| | EMA | RBE2 | Percentage error (%) | CBAR | Percentage error (%) | CWELD | Percentage error (%) |
| 1 | 143 | 160.15 | 11.99 | 159.78 | 11.73 | 160.15 | 1.29 |
| 2 | 232 | 232.15 | 0.06 | 218.79 | 5.69 | 249.31 | 7.46 |
| 3 | 308 | 295.96 | 3.91 | 281.15 | 8.72 | 333.86 | 8.40 |
| 4 | 432 | 406.39 | 5.93 | 380.31 | 11.97 | 413.51 | 4.28 |
| 5 | 437 | 413.68 | 5.34 | 413.18 | 5.45 | 450.60 | 3.11 |
| Total Error | | | 27.23 | | 43.56 | | 24.54 |

Table 5. Mode shapes for EMA and FEA.

| Mode shapes (MS) | Types of modelling | | | |
|------------------|---|---|---|--|
| | EMA | RBE2 | CBAR | CWELD |
| MS 1 |  |  |  |  |
| MS 2 |  |  |  |  |
| MS 3 |  |  |  |  |
| MS 4 |  |  |  |  |
| MS 5 |  |  |  |  |

With regards to modelling joints, all types of model can be modelled when congruent mesh was applied to the model. There is no problem occurred in this study because the FE model was meshed using CQUAD4 for both plates therefore all meshing are congruent and simply coincides with each other. For model updating purpose, RBE2 that represent weld joints do not possess both geometrical and material properties that can be used to update compare to CBAR and CWELD that contains parameters in modelling of weld that can be used to update. From these comparisons, it is found that the characteristic of CBAR is much more appealing compare to other two models, so the CBAR element is selected to represent FSW butt joint modelling and will be proceed to model updating method to improve the correlation between numerical and experimental counterparts.

5.5 FE Model updating of welded structure

Before proceed to model updating, it is essential to make sure the geometrical properties of FE model was well defined because FE model updating only correct the errors that exist from the uncertainties and assumptions of modelling parameters. There are several methods which the model can be parameterized for updating. Seven parameters had been chosen and undergo the sensitivity analysis using SOL200 in MSC Nastran software to select the suitable parameter to update. The sensitivities of the first five natural frequencies were tabulated in Table 6 and comparisons to be made in order to choose the most sensitive parameters.

Table 6. Sensitivity analysis for six parameters.

| Output Type | Young Modulus (E ₇₀₇₅) | Young Modulus (E ₆₀₆₁) | Poisson Ratio (ν ₇₀₇₅) | Poisson Ratio (ν ₆₀₆₁) | Diameter CBAR (D) | Density (E ₇₀₇₅) | Density (E ₆₀₆₁) |
|-------------|------------------------------------|------------------------------------|------------------------------------|------------------------------------|-------------------|------------------------------|------------------------------|
| NF 1 | 40.19 | 39.72 | -8.95 | 8.5 | -0.0008 | -41.06 | -38.67 |
| NF 2 | 54.90 | 54.51 | -8.48 | 8.58 | -23.46 | -52.19 | -47.75 |
| NF 3 | 70.42 | 70.20 | 27.87 | 28.94 | -26.85 | -69.53 | -62.07 |
| NF 4 | 94.92 | 95.28 | -9.08 | 9.06 | -43.51 | -87.94 | -82.46 |
| NF 5 | 102.52 | 104.12 | -11.16 | 10.63 | -0.0005 | -102.35 | -100.32 |

Based on sensitivity data, Young’s Modulus and density for both plates are the most sensitive among all six parameters. But only one of these parameters is selected for updating because of their direct relation in calculation of natural frequency. Modulus of elasticity was chosen because it provides more uncertainties than the density. Diameter of CBAR despite not being sensitive enough is also selected for its contribution for modes 2, 3 and 4. Same goes to Poisson ratio for both materials that sensitive to mode 3 and 5. But to avoid ill conditioning problem, only four parameters was chosen. Therefore only one Poisson ratio was selected due to the same level of sensitivities. In conclusion, four parameters; Young Modulus of AA7075 and AA6061, Poisson ratio for AA6061 involved in model updating. Updating is performed by minimizing the error function and executed on the basis of the first five modes of measured frequencies. Table 7 displays the error between FEA and EMA after updating.

Table 7. Percentage of error between FEA and EMA after updating.

| Modes | Experiment (Hz) | Initial FEA | | Updated FEA | |
|-------------|-----------------|-------------|-----------|-------------|-------|
| | | FEA (Hz) | Error (%) | FEA (Hz) | Error |
| 1 | 143 | 159.78 | 11.73 | 159.77 | 11.85 |
| 2 | 232 | 218.79 | 5.69 | 231.79 | 0.09 |
| 3 | 308 | 281.15 | 8.72 | 300.08 | 2.57 |
| 4 | 432 | 380.31 | 11.97 | 406.22 | 5.97 |
| 5 | 437 | 413.18 | 5.45 | 415.25 | 4.98 |
| Total Error | | | 43.56 | | 25.34 |

From the table, it can be concluded that the natural frequency improved significantly and total error become decreased. It is proved that the modulus of elasticity, Poisson ratio for both plates and diameter of CBAR which are considered as the parameter that significantly affect the behavior of the model. It is also found that not only material properties of the structure influenced the natural frequency of the structure but geometrical properties of CBAR element that used to model the weld joint also plays an important part

that improving the frequency. The changes in value for updated parameters are shown in Table 8.

Table 8. Updated value of parameters.

| Parameter | I | II | Deviation (%) |
|-------------------------------------|---------------|---------------|---------------|
| | Initial value | Updated Value | = (II-I)/I |
| Young’s Modulus, E_{AA7075} [GPa] | 72 | 68.4 | 0.95 |
| Young’s Modulus, E_{AA6061} [GPa] | 69 | 75.3 | 1.09 |
| Poisson Ratio, ν_{AA6061} | 0.33 | 0.35 | 1.06 |
| Diameter CBAR (m) | 0.018 | 0.004 | 0.25 |

6 Conclusions

In summary, this study has deals with some of the technique on modelling the FSW weld joints for prediction of dynamic behaviour. Three types of modelling using RBE2, CBAR and CWELD were developed and the suitability of these three modelling was compared using correlation between natural frequency and mode shapes extracted from EMA and FEA for set E. CBAR element was selected as a reliable model for FSW joints due to its accurate prediction of mode shapes and contains an updating parameter for weld modelling compare to other weld modelling. The model updating was executed in order to improve the correlation between measured counterparts. Before proceed to model updating, sensitivity analysis had been done to make sure the most sensitive parameters will be chosen for model updating. Results show that Young modulus, Poisson ratio for both material and diameter of CBAR are the most sensitive parameter for updating. After perform model updating, total error of the natural frequencies for CBAR model is improved significantly.

The author would like to greatly acknowledge the support by focus group of Advanced Structural Integrity of Vibration Research (ASIVR) and Universiti Malaysia for providing all the equipment used for this project and special thank for Knowledge Transfer Programme (KTP) and Ministry Of Education for financial assistance support.

References

1. B. Gibson, et al. Friction stir welding: process, automation, and control. *Journal of Manufacturing Processes*. **16**(1): p. 56-73 (2014).
2. R. Nandan, T. DebRoy, and H. Bhadeshia. Recent advances in friction-stir welding–process, weldment structure and properties. *Progress in Materials Science*. **53**(6): p. 980-1023 (2008) .
3. D.Lohwasser, and Z. Chen. *Friction stir welding: From basics to applications*. 1st ed., United Kingdom: Woodhead Publishing Limited (2009).
4. J. Guo, J, et al. Friction stir welding of dissimilar materials between AA6061 and AA7075 Al alloys effects of process parameters. *Materials & Design*. **56**: p. 185-192 (2014).
5. P. Sadeesh, et al. Studies on friction stir welding of AA 2024 and AA 6061 dissimilar metals. *Procedia Engineering*. **75**: p. 145-149 (2014).
6. R. Kesharwani, S. Panda, and S. Pal. Multi Objective Optimization of Friction Stir Welding Parameters for Joining of Two Dissimilar Thin Aluminum Sheets. *Procedia Materials Science*. **6**: p. 178-187 (2014).
7. D.M. Neto and P. Neto. Numerical modeling of friction stir welding process: A literature review. *International Journal of Advanced Manufacturing Technology*. **65**(1-4): p. 115-126 (2013).

8. C.C Tutum, and J.H. Hattel. Numerical optimisation of friction stir welding: review of future challenges. *Science and Technology of Welding and Joining*. **16**(4): p. 318-324 (2011).
9. J.E. Gould, and Z. Feng. Heat flow model for friction stir welding of aluminum alloys. *Journal of Materials Processing and Manufacturing Science*. **7**: p. 185-194 (1998).
10. H. Schmidt, J. Hattel, and J. Wert. An analytical model for the heat generation in friction stir welding. *Modelling and Simulation in Materials Science and Engineering*. **12**(1): p. 143 (2004).
11. X. He, F. Gu, and A. Ball. A review of numerical analysis of friction stir welding. *Progress in Materials Science*. **65**: p. 1-66 (2014).
12. N.A. Husain, et al. Finite-element modelling and updating of laser spot weld joints in a top-hat structure for dynamic analysis. *Proceedings of the Institution of Mechanical Engineers, Part C: Journal of Mechanical Engineering Science*. **224**(4): p. 851-861 (2010).
13. M.S.M.Sani, et al. Identification of Dynamics Modal Parameter for Car Chassis. *IOP Conference Series: Materials Science and Engineering*. **17**(1): p. 012038 (2011).
14. V. Infante, et al. Study of the fatigue behaviour of dissimilar aluminium joints produced by friction stir welding. *International Journal of Fatigue*.
15. B. Fu, et al. Friction stir welding process of dissimilar metals of 6061-T6 aluminum alloy to AZ31B magnesium alloy. *Journal of Materials Processing Technology*. **218**: p. 38-47 (2015).
16. S.N. Zahari, et al. Dynamic analysis of friction stir welding joints in dissimilar material plate structure. *Jurnal Teknologi (Sciences & Engineering)*. **78**(6-9): p. 57-65 (2016).
17. J.Fang, et al. *Weld modelling with MSC. Nastran*. in *Second MSC Worldwide Automotive User Conference, Dearborn, MI, USA*. (2000).